Progress In Electromagnetics Research Letters, Vol. 44, 93–99, 2014

Optimizing the Bowtie Nano-antenna for Enhanced Purcell Factor and Electric Field

Jie Yang, Fanmin Kong*, Kang Li, and Jia Zhao

Abstract—With the development of nano-optic technology, the optical nano-antenna has been widely used in the fields of novel light sources, high-sensitive biological sensors, nanometer lithography, and nano-optical imaging. The relationship between the structural parameters of the antenna and the Purcell factor is very important for engineering applications. The electric near field profile of the antenna was calculated and analyzed by using the finite-difference time-domain (FDTD) method, and the influence of the structural parameters on the Purcell factor and the electric field was thoroughly investigated. A careful comparison of bowtie antenna radiation characteristics with different structural parameters was carried out. The results show that the thickness, the length and the curvature radius have great effects on the Purcell factor and the optical antenna's electric near field. These findings are promising for improving the performance of the optical bowtie nano-antenna.

1. INTRODUCTION

Over the past decades, intense renewed effort has been made to understand surface Plasmon polaritons (SPPs) [1]. SPPs are electromagnetic excitations existing at the interface between a metal and a dielectric material [2–4]. The SPPs can confine the electromagnetic energy in sub-wavelength space, which leads to a greatly enhanced localized surface electromagnetic near-field [5]. The physical property of SPPs makes it possible to integrate photonic devices and electronic devices in the nanometer scale [6], which can be applied in fields of new light sources [7], solar cells [8], highly sensitive biosensors [9, 10], nanolithography [11], and nano-optical imaging [12, 13].

In recent years, there has been a surge of research activity on the optical properties of metallic antennas with structures in the nanometer scale. The optical antenna is a nonsocial miniaturization of radio or microwave antenna [14], but the existence of localized surface plasmons (LSPs) in the optical antenna gives it unique behavioral features [15]. Advances in fabrication technique have enabled construction of a metallic nano-antenna in various forms [16–22]. In comparison with the optical antenna composed of metallic particles, the bowtie nano-antenna has wideband characteristics and can be easily fabricated. Since it was proposed as a near-field optical probe in 1997, the bow-tie optical antenna had been applied in biological nano-imaging and near-field optical microscopy. Experiments [23] indicate that near-field enhancement effect and far-field radiation of the optical bowtie antenna are closely related to the antenna's structural parameters. Therefore, exploring the links between them can have a great significance in optimizing the antenna structure. Most theoretical studies on the bowtie antenna have focused on the gap distance [24, 25]. However, the performance of the bowtie nano-antenna can be affected by the size, shape, gap distance, and the incident wavelength. We mainly studied the effect of structural parameters of the bowtie nano-antenna on the Purcell factor and near-field enhancement. The length, flare angle, curvature radius, and thickness were taken into account in our analysis.

Received 16 September 2013, Accepted 6 January 2014, Scheduled 10 January 2014
* Corresponding author: Fanmin Kong (kongfm@sdu.edu.cn).
The authors are with the School of Information Science and Engineering, Shandong University, Jinan, China.

2. ANTENNA MODELS AND COMPUTATIONAL APPROACH

The calculation model is shown in Figure 1. The isotropic, linear, and non-magnetic medium has been considered in the calculation. The optical bowtie nano-antenna consists of two sectors with round tips. The triangular structure has more advantages than the sector structure in local near-field enhancement. However, in the actual production process, the tip of the triangular structure retains a certain curvature due to the limitations of the manufacturing technique. Furthermore, the bowtie structure with a rounded corner has more stable radiation patterns and a smaller area at the same time. The main structural parameters of the optical bowtie nano-antenna selected for simulation are the length L, flare angle θ, curvature radius R, and thickness T, which are shown in Figure 1.

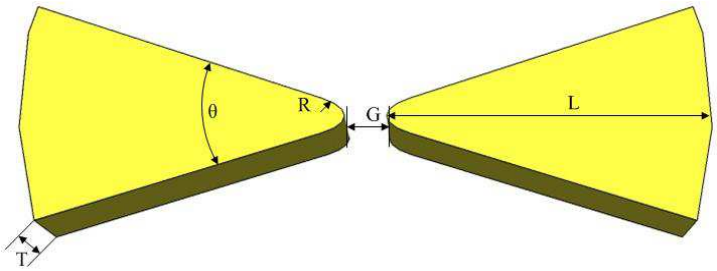

Figure 1. Schematic of the optical gold bowtie nano-antenna.

In order to describe the optical response of the bowtie antenna, a modified Drude dielectric function was employed [26]

$$\varepsilon(\omega) = \varepsilon_\infty - \frac{\omega_p^2}{\omega^2 + j\omega\gamma} \tag{1}$$

where ε_∞, ω_p and $1/\gamma$ stand for the dielectric constant for the frequency going to the infinite, the plasmon frequency and the relaxation time of the metal, respectively. For gold, the parameters used were $\varepsilon_\infty = 9.5$, $\omega_p = 8.948\,\text{eV}$ and $\gamma = 0.06909\,\text{eV}$.

The Purcell factor F used in this study was formulated as (2) [27]

$$F = \frac{\iint P(\theta, \varphi)\, d\Omega}{\iint P_0(\theta, \varphi)\, d\Omega} \tag{2}$$

where $P(\theta, \varphi)$ stands for the power radiated to the far field with the antenna structure, and $P_0(\theta, \varphi)$ is defined as the power radiated to the far field for the reference dipole in a vacuum. The Purcell factor reflects the enhancement extent of the power radiated by the dipole with the optical gold bowtie nano-antenna.

3. RESULTS AND DISCUSSION

To illustrate the influence of geometrical parameters on the Purcell factor and near-field enhancement, the field enhancing properties of the optical gold bow-tie antenna were investigated using finite-domain time difference (FDTD) simulations. In the following calculation, the gap distance was fixed at 20 nm and the incident wavelength was in the range of 400–900 nm.

It is difficult to illustrate the dependence of the Purcell factor on the four different parameters. Therefore, the values L, θ, and R were fixed to constant values. First we investigated the dependence of the Purcell factor on the thickness T of the bowtie nano-antenna, and the result is shown in Figure 2. The peak value of the Purcell factor gradually increased as the thickness decreased. Furthermore, the peak value of the Purcell factor showed a red-shift to the near-infrared region. Electric field enhancement of the bowtie nano-antenna with four different thicknesses is shown in Figure 3. The result showed that

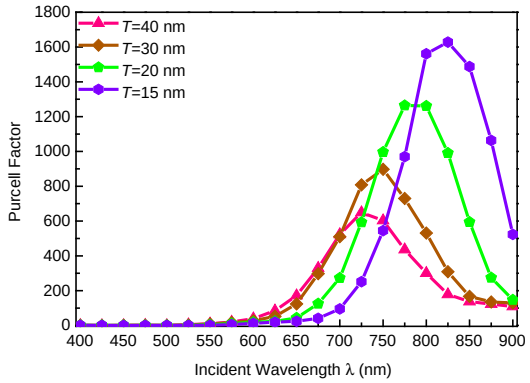

Figure 2. Purcell factor of bowtie nano-antenna with different thicknesses versus incident wavelength, when $L = 100\,\text{nm}$, $\theta = 30°$, and $R = 10\,\text{nm}$.

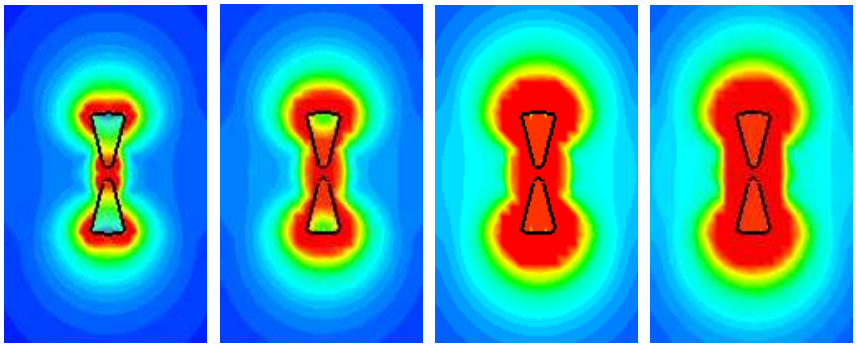

Figure 3. Electric field enhancement of the bowtie nano-antenna with thicknesses of 40 nm, 30 nm, 20 nm and 15 nm ($L = 100\,\text{nm}$, $\theta = 30°$, and $R = 10\,\text{nm}$). (a) $T = 40\,\text{nm}$. (b) $T = 30\,\text{nm}$. (c) $T = 20\,\text{nm}$. (d) $T = 15\,\text{nm}$.

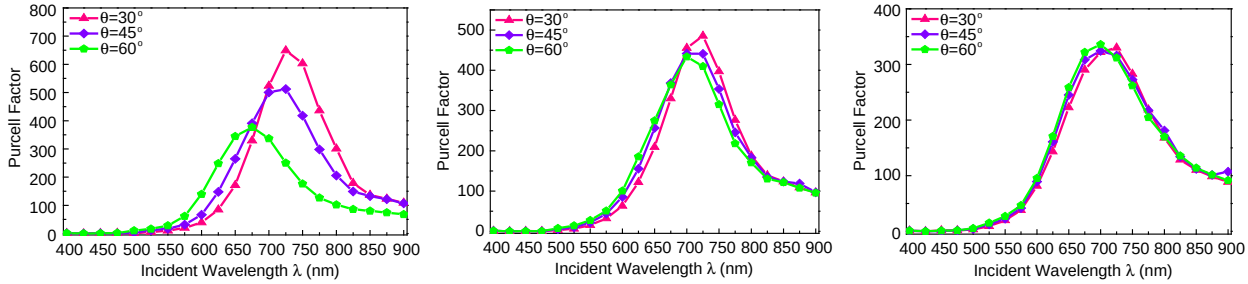

Figure 4. The Purcell factor of the bowtie nano-antenna versus incident wavelength with different flare angles. The curvature radius is (a) 10 nm, (b) 20 nm, and (c) 30 nm.

field enhancement at the sector tip increased while sector thickness decreased. This is because a thinner sector ensures stronger near-field coupling, which leads to a larger fractional plasmon shift.

Next, effects of the bowtie nano-antenna flare angle on the Purcell factor were taken into account, and the simulation results are shown in Figure 4. The flare angle of the bowtie nano-antenna was changed for a constant length L and thickness T. The influence of flare angle on the radiation properties of the bowtie nano-antenna is characterized at $\theta = 30°$, $45°$, and $60°$. The curvature radius was changed from 10 nm to 30 nm for every constant flare angle θ. From Figure 4, it can be seen that the peak value of the

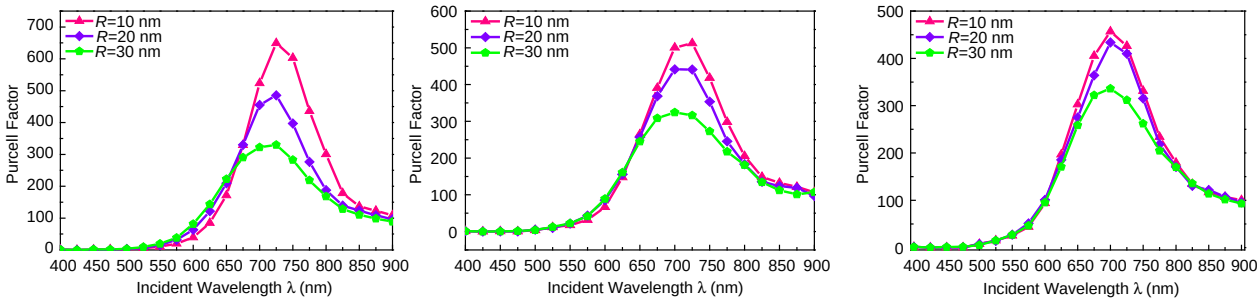

Figure 5. The Purcell factor of the bowtie nano-antenna versus incident wavelength with different curvature radiuses, where (a), (b) and (c) corresponds to flare angles of 30°,45° and 60°, respectively.

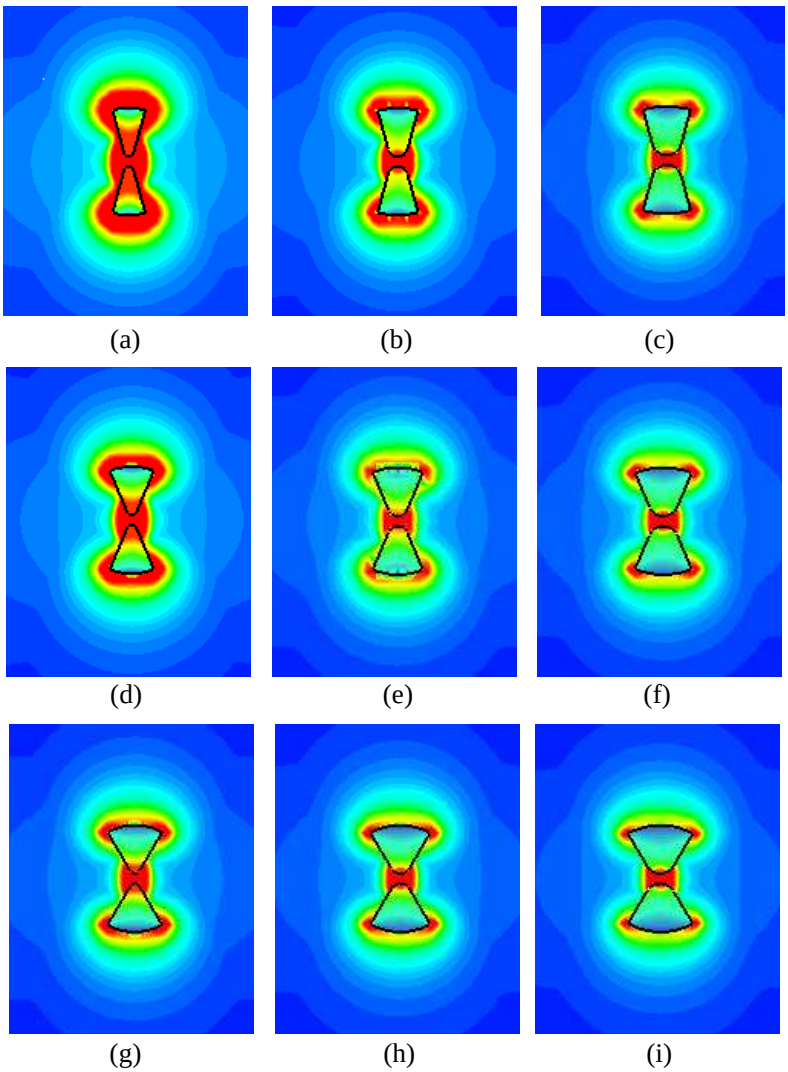

Figure 6. Electric field enhancement of the bowtie nano-antenna with the curvature radius of 10 nm, 20 nm, and 30 nm. (a) $R = 10\,\text{nm}$, $\theta = 30°$. (b) $R = 20\,\text{nm}$, $\theta = 30°$. (c) $R = 30\,\text{nm}$, $\theta = 30°$. (d) $R = 10\,\text{nm}$, $\theta = 45°$. (e) $R = 20\,\text{nm}$, $\theta = 45°$. (f) $R = 30\,\text{nm}$, $\theta = 45°$. (g) R=10 nm, $\theta = 60°$. (h) $R = 20\,\text{nm}$, $\theta = 60°$. (i) $R = 30\,\text{nm}$, $\theta = 60°$.

Purcell factor shows a red-shift in the optical spectrum when the flare angle increased. However, the Purcell factor of the bowtie nano-antenna with a curvature radius of 30 nm was less dependent on the flare angle, which is shown in Figure 4(c). Moreover, the bowtie nano-antenna with a small curvature radius provided a better Purcell factor. This is because the tip of the sector did not change much with the change of the flare angle of the bowtie nano-antenna when the curvature radius became larger. The best peak value of the Purcell factor achieved by the bowtie nano-antenna was 649 at $\theta = 30^\circ$ and at a wavelength of 725 nm.

According to the above analysis, it is obvious that the Purcell factor was remarkably affected by the radius of the curvature. Next, effects of curvature on the Purcell factor were considered. Figure 5 shows the variation of the Purcell factor of the bowtie nano-antenna with different curvature radiuses R. From Figure 5 it can be seen that as R increased from 10 nm to 30 nm, the Purcell factor became smaller, which can be explained by the lighting rod effect theory in electrostatics. According to Rogobete's conclusion, elongated objects should be chosen to benefit from a strong near field at sharp corners [28].

In order to further investigate the effect of curvature radius on the properties of the bowtie nano-antenna structure, the electric field enhancement at a wavelength of 750 nm was investigated. The electric field distribution of the bowtie nano-antenna is shown in Figure 6. A strong electric field appeared on the surface of the bowtie nano-antenna as seen in Figure 6. This is due to the strong local field excited by SPPs. Furthermore, the bowtie nano-antenna with a small curvature radius shows a stronger field than that with a large curvature radius. This may due to the decrease of the charge distribution on the outer side of the bowtie nano-antenna with an increase of the curvature radius of the sector tip.

Resonance behavior of a nano-antenna is highly dependent on the total length of the antenna. Influences of the bowtie nano-antenna's length on the Purcell factor were theoretically investigated. By keeping the thickness, flare angle, and curvature radius constant, the Purcell factor was calculated with different lengths of the bowtie nano-antenna. It can be seen from Figure 7 that the Purcell factor appreciably increased when the length increased from 80 nm to 110 nm, and the peak value of Purcell factor moved toward the greater wavelength side, which means a red shift in the spectrum. This is due to variation of the effective wavelength [29] of the bowtie nano-antenna, which is associated with the physical length of the bowtie nano-antenna. As the physical length of the bowtie nano-antenna becomes larger, the effective resonant wavelength accordingly becomes larger and vice versa. In addition, the increase of the effective resonance wavelength leads to a red shift of the Purcell factor's peak value. To further describe the length of the bowtie nano-antenna associated with the properties of the bowtie antenna, the electric near field intensity of bowtie nano-antenna with different lengths is shown in Figure 8. The results are in agreement with those previously shown in Figure 7. It is clear that electric near field intensity obtains a remarkable enhancement when the length of the bowtie nano-antenna increases from 80 nm to 110 nm in step sizes of 10 nm, as shown in Figure 8.

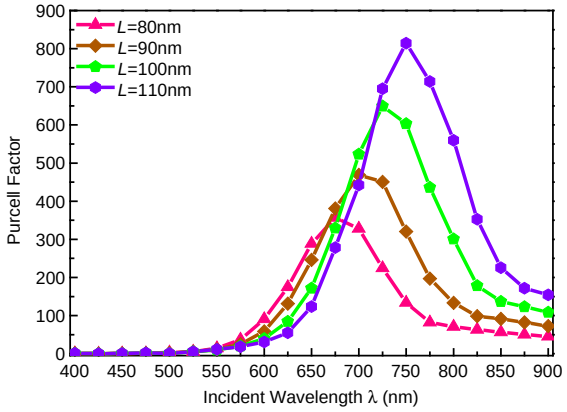

Figure 7. The Purcell factor of the bowtie nano-antenna versus incident wavelength, where the sector flare angle is 30°, the curvature radius is 10 nm and the thickness is 40 nm.

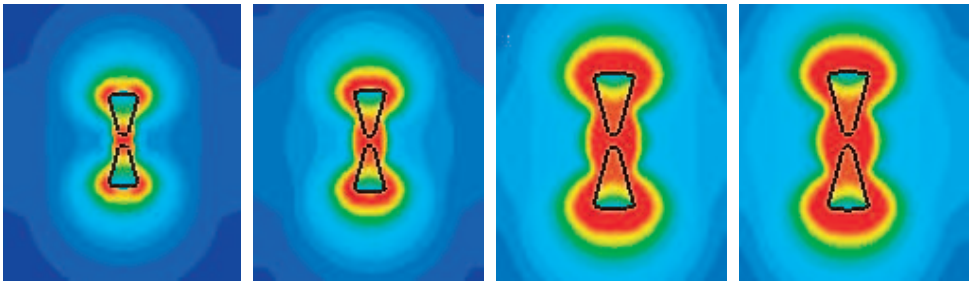

(a) L=80 nm (b) L=90 nm (c) L=100 nm (d) L=110 nm

Figure 8. Electric field enhancements of the bowtie nano-antenna, the length are (a) 80 nm, (b) 90 nm, (c) 100 nm, and (d) 110 nm.

4. CONCLUSION

The bowtie nano-antenna has been shown and analyzed via FDTD simulations. The Purcell factor and near-field enhancement of the bowtie nano-antenna were studied in great details with special focus on the geometrical configuration. The thickness, flare angle, curvature radius, and length were systematically varied in a series of FDTD simulations. A combination of values was found to result in a very high theoretical Purcell factor and electric field enhancement. Also, the internal mechanism for the Purcell factor enhancement and optical bowtie nano-antenna structural parameters were described. These simulated calculation results and corresponding analysis have important significance in designing and optimizing optical bowtie nano-antennas.

ACKNOWLEDGMENT

This work was supported by the National Natural Science Foundation of China (61077043, 61205145) and China Postdoctoral Science Foundation (2012M511506).

REFERENCES

1. Barnes, W. L., A. Dereux, and T. W. Ebbesen, "Surface plasmon subwavelength optics," *Nature*, Vol. 424, No. 6950, 824–830, 2003.
2. Raether, H., *Surface Plasmons on Smooth Surfaces,* Springer, 1988.
3. Ritchie, R., "Plasma losses by fast electrons in thin films," *Physical Review*, Vol. 106, No. 5, 874–881, 1957.
4. Economou, E., "Surface plasmons in thin films," *Physical Review*, Vol. 182, No. 2, 539–554, 1969.
5. Sweatlock, L., S. Maier, H. Atwater, J. Penninkhof, and A. Polman, "Highly confined electromagnetic fields in arrays of strongly coupled Ag nanoparticles," *Physical Review B*, Vol. 71, No. 23, 235408, 2005.
6. Ozbay, E., "Plasmonics: Merging photonics and electronics at nanoscale dimensions," *Science*, Vol. 311, No. 5758, 189–193, 2006.
7. Okamoto, K., I. Niki, A. Shvartser, G. Maltezos, Y. Narukawa, T. Mukai, Y. Kawakami, and A. Scherer, "Surface plasmon enhanced bright light emission from InGaN/GaN," *Physica Status Solidi (A)*, Vol. 204, No. 6, 2103–2107, 2007.
8. Pillai, S., K. Catchpole, T. Trupke, and M. Green, "Surface plasmon enhanced silicon solar cells," *Journal of Applied Physics*, Vol. 101, 093105, 2007.
9. Yadipour, R., K. Abbasian, A. Rostami, and Z. D. Koozeh Kanani, "A novel proposal for ultra-high resolution and compact optical displacement sensor based on electromagnetically induced transparency in ring resonator," *Progress In Electromagnetics Research*, Vol. 77, 149–170, 2007.

10. Mortazavi, D., A. Z. Kouzani, and K. C. Vernon, "A resonance tunable and durable LSPR nanoparticle sensor: Al_2O_3 capped silver nano-disks," *Progress In Electromagnetics Research*, Vol. 130, 429–446, 2012.
11. Shao, D. and S. Chen, "Direct patterning of three-dimensional periodic nanostructures by surface-plasmon-assisted nanolithography," *Nano Letters*, Vol. 6, No. 10, 2279–2283, 2006.
12. Fang, N., H. Lee, C. Sun, and X. Zhang, "Sub-diffraction-limited optical imaging with a silver superlens," *Science*, Vol. 308, No. 5721, 534–537, 2005.
13. Weeber, J.-C., E. Bourillot, A. Dereux, J.-P. Goudonnet, Y. Chen, and C. Girard, "Observation of light confinement effects with a near-field optical microscope," *Physical Review Letters*, Vol. 77, No. 27, 5332–5335, 1996.
14. Park, Q.-H., "Optical antennas and plasmonics," *Contemporary Physics*, Vol. 50, No. 2, 407–423, 2009.
15. Jiang, S.-F., F.-M. Kong, K. Li, and H. Gao, "Study of far-field directivity of optical dipole antenna," *Acta Physica Sinica*, Vol. 60, No. 4, 045203, 2011.
16. Degiron, A. and T. Ebbesen, "The role of localized surface plasmon modes in the enhanced transmission of periodic subwavelength apertures," *Journal of Optics A: Pure and Applied Optics*, Vol. 7, No. 2, S90, 2005.
17. Mühlschlegel, P., H.-J. Eisler, O. Martin, B. Hecht, and D. Pohl, "Resonant optical antennas," *Science*, Vol. 308, No. 5728, 1607–1609, 2005.
18. Taminiau, T. H., R. J. Moerland, F. B. Segerink, L. Kuipers, and N. F. van Hulst, "$\lambda/4$ resonance of an optical monopole antenna probed by single molecule fluorescence," *Nano Letters*, Vol. 7, No. 1, 28–33, 2007.
19. Taminiau, T. H., F. B. Segerink, and N. F. van Hulst, "A monopole antenna at optical frequencies: Single-molecule near-field measurements," *IEEE Transactions on Antennas and Propagation*, Vol. 55, No. 11, 3010–3017, 2007.
20. Panoiu, N. C. and R. M. Osgood, Jr., "Enhanced optical absorption for photovoltaics via excitation of waveguide and plasmon-polariton modes," *Optics Letters*, Vol. 32, No. 19, 2825–2827, 2007.
21. Grober, R. D., R. J. Schoelkopf, and D. E. Prober, "Optical antenna: Towards a unity efficiency near-field optical probe," *Applied Physics Letters*, Vol. 70, No. 11, 1354–1356, 1997.
22. Xie, H., F. Kong, and K. Li, "The electric field enhancement and resonance in optical antenna composed of Au nanoparicles," *Journal of Electromagnetic Waves and Applications*, Vol. 23, No. 4, 534–547, 2009.
23. Wu, Y.-M., L.-W. Li, and B. Liu, "Gold bow-tie shaped aperture nanoantenna: Wide band near-field resonance and far-field radiation," *IEEE Transactions on Magnetics*, Vol. 46, No. 6, 1918–1921, 2010.
24. Bharadwaj, P., B. Deutsch, and L. Novotny, "Optical antennas," *Advances in Optics and Photonics*, Vol. 1, No. 3, 438–483, 2009.
25. Merlein, J., M. Kahl, A. Zuschlag, A. Sell, A. Halm, J. Boneberg, P. Leiderer, A. Leitenstorfer, and R. Bratschitsch, "Nanomechanical control of an optical antenna," *Nature Photonics*, Vol. 2, No. 4, 230–233, 2008.
26. Gao, H., K. Li, F. Kong, H. Xie, and J. Zhao, "Optimizing nano-optical antenna for the enhancement of spontaneous emission," *Progress In Electromagnetics Research*, Vol. 104, 313–331, 2010.
27. Taminiau, T., F. Stefani, and N. Van Hulst, "Single emitters coupled to plasmonic nano-antennas: Angular emission and collection efficiency," *New Journal of Physics*, Vol. 10, No. 10, 105005, 2008.
28. Rogobete, L., F. Kaminski, M. Agio, and V. Sandoghdar, "Design of plasmonic nanoantennae for enhancing spontaneous emission," *Optics Letters*, Vol. 32, No. 12, 1623–1625, 2007.
29. Novotny, L., "Effective wavelength scaling for optical antennas," *Physical Review Letters*, Vol. 98, No. 26, 266802, 2007.